Production of lignocellulosic nanomaterials from thermomechanical pulp fibers: A study of feasibility, tunability, and economic viability

Jaminfaye Reduque

A thesis

submitted in partial fulfillment of the

requirements for the degree of

Master of Science

University of Washington

2026

Committee:

Renata Bura

Richard Gustafson

Anthony Dichiara

Program Authorized to Offer Degree:

Environmental and Forest Sciences

©Copyright 2026

Jaminfaye Reduque

University of Washington

Abstract

Production of lignocellulosic nanomaterials from thermomechanical pulp fibers: A study of feasibility, tunability, and economic viability

Jaminfaye Reduque

Chair of the Supervisory Committee:

Renata Bura

Department of Bioresource Science and Engineering

Lignocellulosic nanofibrils (LCNFs) have gained attention as sustainable nanomaterials due to their unique chemical and physical properties. However, current production methods often rely on costly feedstocks and chemically intensive processes and very few studies investigate ways to adjust the process to achieve tunable properties. In this study, LCNFs were produced from thermomechanical pulp (TMP) using chemical and combined chemical–mechanical treatments. By varying chemical treatment severity and mechanical processing, LCNFs with diverse physical and chemical properties were obtained. A techno-economic analysis (TEA) was also conducted on two treatments that produced LCNFs with similar properties to identify the more suitable approach for future large-scale production. By varying the severity of the chemical treatment through

increasing the number of peracetic acid oxidation pretreatments, a wide range of LCNFs were produced with lignin contents ranging from 3.3%-26.6% and fiber diameters from 52-411 nm. Increased severity of chemical treatment resulted in decreased mass yield from 96.8% to as low as 62.8% due to hemicellulose and lignin loss. Using these LCNFs, thin films were made and tested to further explore the optical and physical properties of the materials. Decreased lignin content led to increased visible light transmittance and decreased sun protection factor and haze. Increased severity of the chemical treatment also decreased average fiber diameter of the LCNFs, accompanied by increased homogeneity, viscosity, elastic modulus, and ultimate tensile strength. Interestingly, the effects of increasing chemical treatment severity on surface wettability were opposing, with reduced fiber diameter leading to lower hydrophilicity and reduced lignin content leading to higher hydrophilicity. Increasing severity of the mechanical treatment, specifically by increasing the number of passes through the microfluidizer, reduced fiber diameters and improved homogeneity, viscosity, surface wettability, elastic modulus, and ultimate tensile strength without altering the chemical composition of the LCNFs.

Based on the TEA, the low-severity chemical/high-severity mechanical treatment process yielded the lowest minimum product selling price (MPSP) for LCNFs, at $5.57/kg assuming a 0% discount rate. By comparison, the high-severity chemical/low-severity mechanical treatment process exhibited a substantially higher MPSP of $9.47/kg under the same assumptions. These results demonstrate that controlled adjustment of chemical and mechanical treatment severity provides a flexible approach for engineering LCNFs with tailored, application-specific properties, while techno-economic feasibility plays an important role in identifying the most suitable

pathway for future large-scale production. Furthermore, the results of this study lay the framework for future studies in LCNF production at commercial scale with other potential feedstocks.

Table of Contents

List of Figures

List of Tables

Acknowledgements

I could not have completed this project without the support of the people and communities around me. Firstly, I want to thank Renata Bura for being with me as my advisor over the last 3 years of my research journey. Under her guidance, I learned and experienced so much more than I thought possible because she knew exactly when and how to push me beyond my expectations. Getting to work with someone who shares your collaboration style, vision and overall passion for environmental change is such a rare and special gift and I feel lucky to have shared that with Renata. She saw what I could achieve as a researcher long before I even stepped foot in a lab and she will never know how much she has changed my life -and the world- for the better.

I would also like to thank the esteemed members of my committee, Richard Gustafson and Anthony Dichiara for their contributions to my project and my growth as a scientist and process engineer. Rick's experience in process design, economic analysis and industry practices helped take my research to the next level, from laboratory experiments to a model for large scale production of sustainable products. I greatly appreciate his guidance and patience as I navigated concepts that were so outside of my comfort zone. Anthony's vast knowledge of all things material science was an incredibly valuable resource in all phases of my research from experimental design and troubleshooting to interpretation of my results. I can't thank him enough for the generosity in his teaching and the learning opportunities he provided for me and so many others.

I also want to thank the rest of the faculty and staff of the BSE (now SBSE) department at UW for their unwavering support of me and the program that I am proud

to call home. Heidi Gough, Mutian Hua and Ed Draper have all impacted me and my career trajectory in different ways. They, along with my committee, have worked tirelessly to bolster the growth of the program and expand opportunities for the students to new heights. Their dedication to the students shows in every classroom, laboratory, meeting, and recruitment event and the fruits of their labor will be engineers that will go on to create solutions to some of the world's biggest environmental challenges.

The BSE program has given me so much, not only the knowledge I gained in class but also the people I met who enriched my whole experience. Thank you to my friends and colleagues Lexi E., Lexi M., Anna, Dylan, Jack, Greg and Abhi for their valuable collaboration and for making such a difficult journey more bearable each day. I also want to thank the undergraduate students, Cate Blaes and Alaina Duque, for their contributions to my research and for all the laughs and chats we shared during Klason. Special thanks to Kurt Haunreiter for his time as the Wollenberg lab manager and for setting the basis for my passion for nanocellulose, I would truly not be here without his support.

I want to thank Giselle Wyers, Geoffrey Boers, Serena Chin, and the entire University of Washington Choral program. I couldn't not have made it through the last 6 years of schooling without the creative outlet of singing to balance my STEM intensive course load. My time in the University Chorale, Chamber Singers and Concord Chamber Choir have given me so many amazing performance opportunities and long-lasting relationships that I will cherish forever. Choir is a community that has served me my entire life, and I plan to return the favor going forward.

Thank you to my parents, Benjamin and Imelda Reduque, my siblings, Jireh and Jiemyjoyce Reduque and our fluffy dog Milo. They are the reason I am here today and every sacrifice they've made for me is the motivation behind the work that I do. Their support means everything to me and drives me to make them proud every day. Salamat sa lahat, mahal na mahal kita.

Lastly, I want to thank the amazing people that I get to call friends, Ruby, Sarah, Lainey, Cole, Charlie, Cameron, and Matt, for their overwhelming support over the years. Their unconditional love and care for me have kept me going in some of the most difficult points of school and life. My relationships with each person are so special to me and it means the world that I can lean on any one of them when I need support. I also want to thank my friends/co-parents, Ki'i and Aidan, for being amazing roommates and friends and for taking such good care of our puppy Chirashi. Finally, I want to thank my partner Nick for his support for me over the last year. His love and care showed up for me in every meal he made me when I had to write, every thoughtful comment and edit he made on my manuscript and every time he listened to me rant about things going wrong in the lab. He has always been there to remind me that I am capable of achieving great things and I could not have done it without him.

Dedication

To Evan, Dallin, Jon, Aaron, Kai, Juniper and all the ones we lost too soon.

1. Introduction

1.1. Lignocellulosic nanofibrils (LCNFs)

Lignocellulosic nanofibrils (LCNFs), also referred to as nanofibrillated cellulose (NFC) or nanocellulose, are cellulose fibers with diameters within 1 to 100 nanometers and consist of cellulose, hemicellulose, and lignin [1]. LCNFs have impressive mechanical properties, reinforcing capabilities, low density, and biodegradability making them ideal for use in sustainable material applications [1]. Cellulose is the most abundant biopolymer found in nature where it provides structural strength to all kinds of plants [2]. Various feedstocks have been used to produce LCNFs including wheat straw, sugar cane, corn stover, and sawdust to name a few [3–5]. One potential feedstock for LCNF production is thermomechanical pulp fiber.

1.2. Thermomechanical pulp (TMP) fibers

The process of making fibers from thermomechanical pulping (TMP) starts with treating wood chips with high temperature (115-155°C) and high pressure (20-40 psi) steam to soften the lignin and enhance fiber separation [6]. They are then refined at high pressure, and at a temperature that is just under the glass transition for lignin (140°C) so that fiber separation in the middle lamella layer of the cell wall can occur [6]. Because there is no delignification involved in making TMP fibers, the process has a high fiber yield of 80-90% and the resulting fibers maintain high lignin and hemicellulose content [7]. Several TMP mills exist across the Pacific Northwest most prominently in Washington and Oregon [8–10]. TMP fiber is traditionally used for packaging materials and paperboard in addition to furnishing for newsprint, magazines, and printing paper [6]. TMP fiber is an attractive starting material for the production of sustainable cellulose-

based nanomaterials because it is already fractionated but still retains its raw material chemical composition.

1.3. Nanocellulose made from thermomechanical fibers

Only a few studies in the literature demonstrated the production of LCNFs/CNFs from TMP fibers. These studies typically employed either purely mechanical treatments or a combination of mechanical treatment with chemical pretreatment to produce LCNFs exhibiting varying chemical and physical properties [11–15].

1.3.1. Mechanical methods of producing TMP fiber nanocellulose

LCNFs can be made from TMP fibers using mechanical treatment. Vergara-Figueroa et al. used a one-step micro grinding treatment by running TMP fibers made from radiata pine through a super masscolloider with a disc opening of 0.5 μm to produce TMP-NF or thermomechanical pulp nanofibers [11]. The sample was run for 2 continuous hours at 1500-1800 rpm at 10% w/v consistency [11]. After centrifugation for 30 min 12,000 rpm, the supernatant was collected and called TMP-NF [11]. The TMP-NF was observed to have a high lignin content of 32%, cellulose content of 45%, hemicellulose content of 16%, 5% extractives and, 1% ash [11]. Analysis of fiber morphology showed that the fibrils had an average diameter of 35 ±13 nm [11]. The TMP-NF fibers were also dried into pure LCNF films that were hot pressed at 75˚C for 24 hours [11]. The films showed a higher contact angle of 71˚-85˚ compared to similar films of pure cellulose (~60˚) meaning that they are less hydrophilic, likely due to the higher lignin content in the TMP-NFs [11]. Additionally, the TMP-NF films had lower elastic modulus, meaning they were more flexible [11]. Overall, the TMP-NF films showed promising mechanical and barrier properties for potential food packaging applications.

In work by Serra-Parareda et al., TMP fibers made from pine were disintegrated and then refined using a Valley beater with a 60-minute residence time. The refined pulp was then subject to varying levels of microfluidization with increasing pressures (300, 600, and 900 bar) and number of passes at each stage (1-3 passes) [16]. The results showed increased nanofibrillation yields, from 3.1% for unhomogenized fibers to 8.1% for fibers treated with three passes at each pressure stage, as determined gravimetrically by centrifugation and separation of the supernatant as the nanofibrillated fraction[16]. When the viscosity was measured over a range of shear rates, the LCNFs demonstrated shear thinning behavior and samples that were treated with more severe homogenization had higher viscosities [16].

Osong et al. used two processes of producing nanocellulose, both by isolating and collecting TMP fines using mesh screens [12]. The first method was a standard procedure using a Bauer-McNett Classifier which forces a sample suspended in water through a series of screens of increasingly small mesh sizes [12]. This process required a continuous flow of water to prevent the screens from clogging and to keep the fibers constantly mixing [12]. The second method was invented by the authors where the TMP was disintegrated for 30,000 revolutions, diluted with water, and forced through a mesh wire screen with the help of an agitator [12]. Fines from each process were homogenized using high pressure to produce “nano-ligno-cellulose" [12]. Osong et al. reported fibril diameters after homogenization between 80-115 nm and demonstrated that LCNFs could be produced from TMP without chemical pretreatment [12].

Treating TMP fibers solely with mechanical treatment presents challenges when considering commercial-scale production of TMP-LCNFs. The process proposed by

Vergara-Figueroa et al. of extensive microgrinding uses a substantial amount of energy to achieve fibrils of nanometer dimensions [1,11]. Additionally, the process used by Osong et al. uses a large amount of water to operate [12]. While successful production of LCNFs from TMP fibers was achieved using solely mechanical methods, neither process is economically viable due to potentially high operating costs [11,12].

1.3.2. TMP fiber nanocellulose synthesis with TEMPO Oxidation

The most common chemical treatment method for producing nanocellulose is TEMPO-mediated oxidation. It uses a 2,2,6,6-tetramethylpiperidine-1-oxyl (TEMPO) radical in combination with an oxidizer, usually sodium hypochlorite (NaClO), to produce nanocellulose with very little residual lignin and hemicellulose and a high surface charge [13].

This method was used on bleached chemi-thermomechanical pulp (BCTMP) derived from aspen, a hardwood, by Bakkari et al. in combination with mild mechanical treatment to produce cellulose nanofibers (CNF) [13]. TEMPO and NaBr were first added to the fibers, followed by the dropwise addition of the oxidant, NaClO, while maintaining the pH at 10.5–11.5 [13]. The fibers were then washed thoroughly and defibrillated using a super masscolloider to produce a cellulose nanofiber suspension [13]. The resulting fibers had a lignin content of 6%, a hemicellulose content of 9%, and the yield for the process ranged from 51% to 77% [12]. The CNFs also had a 1440 μmol/g carboxylate content which resulted in high water retention. This was significant for applications in cement and concrete fillers for purposes of better flow control and reduced crack propagation [13].

The effects of TEMPO on chemical versus enzymatic oxidation were explored by Jiang et al. using softwood TMP fibers [17]. Reactions of TEMPO/NaBr/NaClO and TEMPO/Laccase/O2 were performed on TMP fibers individually and then the oxidized fibers were mechanically disintegrated using an ultrasonic homogenizer [17]. The novel TEMPO/NaBr/NaClO process produced CNFs with a carboxylic acid content of 1600 μmol/g and 5% residual lignin [17]. Comparatively, the enzymatic TEMPO treatment TEMPO/Laccase/O2 produced CNFs with 15% lignin and 1800 μmol/g carboxylate contents [17]. Average fibril diameters ranging from 3-10 nm were reported [17].

TEMPO mediated oxidation produces high-quality nanocellulose that is well suited for high-value applications, such as medical or pharmaceutical sectors. However, large-scale production is limited due to the high capital and operating costs associated with the TEMPO oxidation process, as well as its low yield resulting from the removal of lignin and hemicellulose [13,14,17]. Additionally, TEMPO is a very harsh oxidant that is difficult to recycle and can be toxic if released into the environment [18]. As environmental awareness and concern continue to grow, developing greener methods for LCNF production has become an increasingly important area of research.

1.3.3. Other chemical treatments for production of nanocellulose from TMP fibers

Jiang et al. demonstrated that nanocellulose can be produced from softwood TMP fibers using an acidic deep eutectic solvent (DES) technique [14]. The TMP fibers were first freeze dried, then reacted at 90˚C for 6 hours, followed by water dialysis, and subsequently mechanically fibrillated with a kitchen blender at 3000 rpm for 15 minutes [14]. This process yielded LCNFs with a 57% yield, 32.6% lignin content, and reported diameters between 5-8 nm [14]. While DES pretreated fibers exhibited good uniformity

and were produced using recyclable chemical alternatives to traditional TEMPO oxidation, the process involved multiple steps and has not been demonstrated at a scale beyond laboratory production [14].

Enzymatic hydrolysis of TMP fibers has been shown to produce LCNFs as a byproduct of sugar production [15]. In one study, bleached chemi-thermomechanical pulp derived from mixed softwoods was subjected to neutral sulphonation, followed by hydrolysis using cellulase cocktail Cellic CTec 3 at 50˚C for 12 hours [15]. The results showed that 22% of the fibers were fully hydrolyzed to monosaccharides and 29% was recovered as LCNFs [15]. The resulting LCNFs had high lignin content (26.8%–38.5%) and had diameters ranging from 7.1 to 7.6 nm [15]. Transparent films made from these LCNFs exhibited a high water contact angle of 82.8˚ [15].

While this study demonstrates the potential for parallel sugar and LCNF production from TMP fibers via enzymatic hydrolysis, the LCNF yield remains relatively low, and the use of enzymes presents challenges for scalability in industrial applications.

1.3.4. Proposed method of producing lignocellulosic nanofibrils (LCNFs) from TMP fibers

Literature has shown that a combination of alkaline peroxide fractionation and peracetic acid (PAA) oxidation is an effective chemical treatment for the production of lignocellulosic nanofibrils when combined with mild mechanical treatment. Pascoli et al. demonstrated the robustness of this chemical pretreatment process by successfully applying it to a wide variety of agricultural residues, including wheat straw, reed canary grass, corn stover, and industrial hemp [3,4]. The biomass was first fractionated using alkaline peroxide fractionation for 150 minutes at 90°C, then subjected to a single PAA

oxidation at pH 4.8 and 85˚C for 45 minutes, followed by blending. The solutions were then centrifuged to separate larger fractions of fibers which were then further homogenized using a microfluidizer. This process produced LCNFs with diameters ranging from 2.1-2.8 nm and 7% lignin content [3]. Pascoli's process using wheat straw has been evaluated through techno-economic analysis (TEA) to explore its commercial feasibility. TEA showed a breakeven selling price of US$3.83/kg and an outstanding selling price of US$4.60/kg at a 15% discount rate [19]. Main cost reductions were driven by the use of agricultural residues as a feedstock, low cost chemicals, and moderate capital and operating costs by mild operating conditions and use of common unit operations [19].

PAA oxidation was also demonstrated to be effective on woody biomass by Yang et al [20]. In their study, spruce matchsticks of 2 mm diameter were subjected to four rounds of PAA oxidation using a method similar that of Pascoli et al., followed by fibrillation in a kitchen blender [4,20]. The fibers were centrifuged to separate larger fibers, unfibrillated material, which was collected and blended again. After two rounds of sediment recovery, the overall yield was approximately 55% [20]. The resulting LCNFs had a high hemicellulose content of 30%, low lignin content of 2% and fiber diameters of less than 5 nm [20].

TMP fiber is a promising starting material for this process because its chemical composition closely resembles that of raw woody biomass, and it has already been physically fractionated, making it more amenable to chemical pretreatment. Based on the study by Yang et al. it is known that the PAA oxidation process can be applied to woody biomass to produce lignocellulosic nanofibrils [20]. In this study, LCNFs were

produced from TMP fibers using Pascoli's method of alkaline peroxide fractionation and peracetic acid oxidation as a pretreatment step prior to mechanical fibrillation and subsequent homogenization [4]. Additionally, Serra-Parareda et al. demonstrated that TMP fibers can be microfluidized without chemical pretreatment to further reduce fiber size, highlighting the potential of mechanical processing alone to induce fibrillation [16]. We hypothesize that high-yield LCNFs retaining cellulose, hemicellulose, and lignin can be produced using a widely available, low-cost feedstock and an eco-friendly chemical treatment. Success in this study could pave the way for the commercial production of lignocellulosic nanofibrils and their use in sustainable bioproducts, such as biodegradable plastics and food packaging.

2. Objectives

i) Assess the feasibility of delignification and peracetic acid oxidation on thermomechanically pulped fibers to produce lignocellulosic nanofibrils.

ii) Explore combinations of chemical and mechanical treatments to produce various grades of nanocellulose with tunable chemical and physical properties.

iii) Model the processes at a commercial scale and conduct techno-economic analysis (TEA) to assess its potential for large scale production.

3. Methods

3.1. Materials

TMP fibers were obtained from Inland Empire in Spokane, WA. The TMP pulp was a mixture of softwoods (Western Hemlock, Grand Fir and some other pine and spruce species) that have been bleached using hydrogen peroxide, sodium hydroxide

and sodium silicate with little to no lignin removal. The sample was stored in a cold room until use and was thoroughly washed with nanopure water to remove storage preservative.

3.2. Alkaline peroxide fractionation

TMP fibers were fractionated by alkaline peroxide treatment at 87°C for 150 minutes in a glass jacketed reactor equipped with a high shear mixer, set at 5000 rpm, and a heater to circulate water at a constant temperature. The fibers were combined with 15% sodium hydroxide, 7.5% hydrogen peroxide, 0.15% DTPA, 0.3% pulping surfactant and deionized water to bring the solution to 2.5% consistency. After fractionation, the fibers were vacuum filtered then thoroughly washed with deionized water.

3.3. Peracetic acid oxidation

Fractionated TMP fibers were refined in a PFI mill for 30,000 revolutions – with freeness of about 35- then treated with a 30% w/w charge of PAA to fiber at pH 4.8, at 85˚C for 50 minutes at 5% consistency using a rotovap with a water bath that was turning at 25 rpm to ensure even heat and chemical distribution. The reaction was then filtered and quenched with 2 L of 0.02 M sodium hydroxide for 2 hours, then washed with DI water until the wash water was neutral in pH and conductivity. This PAA reaction, quench, and washing process was carried out on 5 different batches of TMP fiber to produce samples each with a different number of PAA treatments as summarized by **Table 1**. The PAA treated fibers were then mechanically fibrillated using a kitchen blender at 0.4% consistency for 30 minutes to produce LCNFs then stored in glass bottles at 3˚C until use.

3.4. Homogenization

Homogenization of select samples of blended LCNFs was carried out with a Microfluidics LM20 microfluidizer at 0.4% consistency and 30,000 psi. F-1Ox and 1Ox samples were treated with 5 passes through the homogenizer and 4Ox sample was treated with 1 pass as shown in **Table 1**.

Sample ID	Treatment summary
TMP	No treatment
F	Fractionation
F-1Ox	Fractionation, 1 oxidation at 30% PAA
1Ox	1 oxidation at 30% PAA
2Ox	2 oxidations (the first at 30% PAA, then 15% PAA)
3Ox	3 oxidations at 30% PAA
4Ox	4 oxidations at 30% PAA
F-1Ox5H	Fractionation, 1 oxidation at 30% PAA, 5 passes of homogenization
1Ox5H	1 oxidation at 30% PAA, 5 passes of homogenization
4Ox1H	4 oxidations at 30% PAA, 1 pass of homogenization

Table 1. *Summary of sample chemical and mechanical treatments.*

3.5. Lignocellulosic nanofibril films

LCNF films were solution cast in 100 mm diameter glass crystallizing dishes with 10 wt.% ethanol and 125 g total solution. The samples were dried in an NRTL-certified vacuum oven at 60 °C and -25 mmHg for approximately 60 hours then removed from the oven once consistency was gel-like (when remaining solution was ~40-60 g) to finish drying at room temperature and pressure in a fume hood. The oven was equipped with a digital controller and connected to a 240 L/min rotary vane vacuum pump with

an exhaust filter, KF25D adapter, and clamp. After drying, the films were hot-pressed using a Rosin Tech heat press at 145 °C for 15 hours. All films were then conditioned at 23 °C and 30% relative humidity for at least 12 hours before testing.

3.6. Characterization Methods

3.6.1. Mass yield after oxidation

Total mass yield after oxidation was determined gravimetrically by comparing the oven-dry mass of the final fibers to that of the original TMP feedstock.

3.6.2. Chemical composition

Klason chemical analysis was performed on the original TMP fibers, fractionated fibers (F) and all fibers after PAA oxidation (F-1Ox, 1Ox, 2Ox, 3Ox, and 4Ox). The samples were ground and mixed with 72% sulfuric acid for 2 hours then autoclaved to monomerize the cellulose and hemicellulose. The solution was then filtered to separate precipitated acid insoluble lignin (AIL) and dissolved acid soluble lignin (ASL). ASL was analyzed using UV-spectrophotometry and AIL was weighed and both were combined to equal total lignin content of the sample. Cellulose and hemicellulose content were characterized using Shimadzu High Performance Liquid Chromatography (HPLC). Ash content was measured gravimetrically by measuring the mass of ground PAA treated sample before and after 12 hours in a 575˚C oven. Total extractives were measured via water based Soxhlet extraction for 12 hours.

3.6.3. Fourier-transform infrared spectroscopy (FTIR)

Infrared spectra data was collected using a Shimadzu FT-IR Prestife-21 spectrometer with a DLATGS detector and a MIRacle ATR accessory from PIKE

Technologies. Data was collected at ambient conditions over the 500–4000 cm^{-1} range, with a resolution of 4 cm^{-1} and 40 accumulated scans.

3.6.4. Surface charge density

Surface charge density was measured using conductometric titration in which an excess of HCl was added to 50 mL of 0.1% consistency suspension of PAA treated fiber to fully protonate available groups on the fiber, then titrated with 0.01 M NaOH in 100 µL increment while conductivity was measured populated onto a curve. Using the curve to identify two inflection points, charge density [µmol carboxyl/ g fiber] was calculated using the equation below where V1 is the volume of NaOH added to neutralize the HCl and V2 is the volume needed to neutralize the carboxylic acids.

$$Charge\ density\ = \frac{(V1 - V2) \times [NaOH]}{Oven\ Dry\ Sample\ Mass}$$

3.6.5. Viscosity

Viscosity of LCNFs at 0.4% consistency was evaluated using a TA Rheometer HR-20 fit with a stainless-steel Peltier heating plate, 20.0 mm parallel plate geometry and a 1 mm geometry gap. Viscosity was measured at a held temperature of 25˚C, over shear rates of 0.001-1000 s^{-1} with 5 measurements taken per decade for a total of 35 minutes per run.

3.6.6. Scanning electron microscopy (SEM)

LCNFs were probe sonicated for 4 minutes at maximum amplitude then diluted to 0.005% consistency. The dilute sample was then dropcast onto a silicon wafer and dried using a hot plate. The sample was sputter-coated with 2 nm platinum using a

Leica EM ACE600 coater then imaged using an Apreo S scanning electron microscope equipped with an ETD in chamber and T2 SE detector. The images were analyzed using ImageJ software by collecting n=500 representative diameter measurements and calculating average diameter, standard deviation and % of fibers under 100 nm.

3.6.7. X-Ray Diffraction (XRD)

Crystallinity index was evaluated using X-ray diffraction (XRD) on a Bruker D8 Discover system with a Pilatus 100K 2D detector and Cu Kα radiation, operated at 50 kV and 1 mA. Diffractograms of neat films were collected over a 2θ range of 10°–48° in 5.5° increments. The crystallinity index (CI) was calculated using the Segal method, where I_t is the intensity of the crystalline (2 0 0) peak at 2θ = 22.7°, and I_a is the intensity of the amorphous (1 1 0) peak at 2θ = 18°, as shown in the equation below.

$$CI\ (\%) = \frac{I_t - I_a}{I_t} \times 100$$

3.6.8. UV-vis spectroscopy

The optical transmittance was measured using a PerkinElmer UV/VIS/NIR Lambda 750 spectrometer across a wavelength range of 250–800 nm. Visible light transmittance was evaluated by recording percent transmittance at 660 nm and 360 nm was used to assess transmittance in the UV-B and UV-A region. Light transmittance in the visible range was standardized by film thickness by calculating the attenuation coefficient according to the Beer-Lambert law [21]. Sun protection factor (SPF) was calculated using the Mansur equation below where *EE* is the erythemal effect spectrum, *I* is the solar intensity and *Abs* is the UV absorbance [22]. *EE x I* are constants that have been determined from 290-320 nm, in 5 nm increments [22]. Optical haze was also

measured using the same spectrometer over a range of 380–780 nm according to ASTM D1003 standard haze procedure [23]

$$SPF = 10 \times \sum_{290}^{320} EE \times I \times Abs$$

3.6.9. Thermogravimetric analysis (TGA)

Thermal properties were assessed using a Mettler Toledo TGA/DSC 3+ thermogravimetric analyzer. Samples were heated from room temperature to 600 °C at a rate of 10°C/min under a nitrogen flow of 60 mL/min.

3.6.10. Surface wettability and surface free energy

Using a Krüss Drop Shape Analyzer, surface wettability was assessed by measuring the static contact angles of water and diiodomethane on film surfaces. Images were captured immediately after droplet deposition. Surface free energy was calculated using the Owens-Wendt-Rabel-Kaelble (OWRK) model.

3.6.11. Tensile testing

Mechanical properties were measured using a Thwing-Albert EJA Vantage-10 Tensile Tester with a 50 mm gauge length and 15 mm strip width. All films were conditioned for at least 12 hours at 50% relative humidity and 23.0°C in accordance with TAPPI standard T402. Thickness measurements were taken at 10 points per film strip using a Digimatic Micrometer.

3.6.12. Techno-economic analysis (TEA)

Processes for 1Ox5H (the low-severity chemical/high-severity mechanical treatment) and 4Ox1H (the high-severity chemical/low-severity mechanical treatment)

were chosen for techno-economic analysis (TEA) comparative study because they produce fibrils with similar morphologies and represent the most mechanically intensive process and the most chemically intensive process respectively. Capital and operating production costs for each process were estimated using Microsoft Excel spreadsheets based on laboratory results and mass and energy balances. Definition of process areas and estimations of capital and operating costs were derived similarly to the TEA performed in Pascoli et al. on the commercial production of LCNFs from wheat straw [19]. The facility includes onsite PAA production, PAA reaction and washing (1 area per round), mechanical fibrillation, homogenization (1 area per pass) and wastewater treatment (scaled with rounds of PAA). Capital costs were based on equipment prices found in the literature, online, from vendors and other sources and scaled up using the appropriate facility size ratio and scaling exponents found in literature to achieve a model with a basis of 100 T of TMP fibers per day (oven dry). Total direct costs (TDC) include equipment installation, site development, piping and wastewater treatment facility. Total indirect costs (TIC) include proratable expenses, field expenses, office construction and other expenses relating to start-up. The sum of TDC and TIC results in the fixed capital investment (FCI) and a working capital of 5% of the FCI was assumed. Total capital investment (TCI) is calculated as the sum of the FCI and working capital. Fixed operating costs were also considered including all labor expenses, maintenance, operating supplies and property insurance. Variable operating costs include feedstock, chemicals and utilities necessary to run each process. Prices of chemicals and utilities were acquired from Pascoli's TEA [19].

Minimum product selling price (MPSP) was calculated using a discounted cash flow analysis in Microsoft Excel by calculating the internal rate of return (IRR) with discount rates of 0% (break-even point), 7%, 15%, and 20%. Due to the general unpredictability of the corporate tax environment, a pre-tax financial position was assumed. Other major assumptions are summarized in **Table 2** below.

Parameter	**Values**
Operating days	350 days/year, 24 hours/day
Production capacity in year 0	0%
Production capacity in year 1	50%
Production capacity in years 2+	100%
Financial horizon	10 years
Number of employees/process area/day	4
Discount rates	0%, 7%, 15%, 20%
Equity financing	60%

***Table 2**. Main parameters used in the discounted cash flow analysis.*

4. Results and Discussion

4.1. Effect of process conditions on feedstock oxidation

TMP fibers were given an alkaline peroxide fractionation treatment in a high shear mixer at 87˚C. The fractionated fibers (F) were treated with a single PAA oxidation at 30% w/w PAA to fiber charge (F-1Ox). Additionally, washed and untreated TMP fibers were subjected to four different PAA oxidation treatment conditions (see **Table 1**) and will be referred to as 1Ox, 2Ox, 3Ox and 4Ox to reflect the extent of their oxidation treatment. The products for each process were analyzed using Klason chemical analysis, ash analysis and Soxhlet extraction to characterize the lignin, carbohydrate, ash, and extractive contents. **Table 3** below summarizes the chemical

composition of the original bleached TMP fibers, fractionated TMP fibers and all oxidized fibers, along with corresponding mass balances.

Mass yield for F was 94.7% with hemicellulose recovery of 85.1 % and 0.0% lignin removal. Similarly minimal removal of about 0% lignin observed by Alvarez-Vasco et al. where Douglas fir chips were given alkaline peroxide treatment at 90°C and 140°C [24]. They did however observe significant lignin removal of up to 22% with alkaline peroxide treatment at 180°C indicating that a much higher temperature is required for alkaline peroxide treatment to effectively delignify softwood biomass [24]. Due to the lack of lignin removal after alkaline peroxide treatment, and greater removal of lignin during peracetic acid oxidation, more severe chemical treatments with PAA oxidation were explored based on work by Yang et al. in which spruce match sticks were treated with peracetic acid oxidation 4 times to produce CNFs [20].For 1Ox-4Ox samples, overall mass yields ranged from 62.8% to 92.4% across treatments, decreasing with increasing number of oxidation treatments. Yang et al. reports a yield of 55% for their CNFs produced from 4 PAA treated spruce match sticks after centrifugation to separate larger wood fragments [20]. Cellulose recovery ranged from 88.0% to 96.8%. Hemicellulose recovery ranged from 71.5% to 95.9%. With increasing chemical treatment, hemicellulose and cellulose recovery decreased. Delignification ranged from 16.7% to 92.1% and showed a positive correlation between number of PAA oxidation stages and delignification.

Increasing number of oxidation treatments reduced lignin contents from 26.6% in the untreated biomass to as low as 3.3%, accompanied by an increase in both cellulose content from 51.1% to 71.5% and hemicellulose content from 9.7% to 11.1%.

This result is not surprising as peracetic acid, a known bleaching agent, has been shown to selectively delignify lignocellulosic biomass [25]. This is done most predominantly by the oxidation of guaiacyl units found commonly in softwood lignin, causing the phenolic rings to open and form fumaric and maleic acid derivatives [26]. Lignin contents for F-1Ox and 1Ox samples were not statistically significantly different (α=0.05) which further supports that the alkaline peroxide pretreatment did not affect the lignin in the original TMP. Fibers treated with 4 rounds of PAA oxidation in this study had a lignin content of 3.3% which is greater than the 2% lignin content reported by Yang et al. after 4 consecutive PAA treatments on spruce matchsticks [20]. Hemicellulose content however was lower ranging from 9.7% to 11.1% compared to Yang et al. with 30% after 4 PAAs [20]. It should be noted that literature values for softwood chips of species found in the TMP used for these experiments (hemlock, fir, pine, spruce) range from 18.1% to 24.0% [27]. From this, it can be deduced that around 54-60% of the hemicellulose was removed during the TMP and peroxide bleaching process. Alkaline peroxide conditions have been shown to cause hemicellulose loss as the glucomannans are degraded in oxidation [24]. Ash and extractives content remained consistently low among all samples ranging from 1.2% to 2.2% for ash and 2.9-6.5% for extractives.

	Chemical composition (%)					Mass balance (%)			
	Cellulose	Hemicellulose	Lignin	Ash	Extractives	Mass yield	Cellulose recovery	Hemicellulose recovery	Lignin removal
TMP	51.1 ± 0.6	9.7 ± 0.1	26.6 ± 1.0*	1.2 ± 0.0	4.2 ±0.0	-	-	-	-
F	54.9 ± 1.3	8.7 ± 0.1	28.3 ± 0.7*	1.4 ± 0.2	2.9 ± 0.2	94.7	101.8	85.1	0.0
F-1Ox	58.8 ± 0.6	9.0 ± 0.1	23.3 ± 0.2*	1.4 ± 0.3	4.2 ± 0.4	95.9	101.6	97.6	21.8
1Ox	53.5 ± 0.4	10.1 ± 0.0	24.0 ±0.3*	1.9 ± 0.0	4.5 ± 0.4	92.4	96.8	95.9	16.7
2Ox	57.8 ± 0.7	10.5 ± 0.1	16.3 ± 2.0	2.2 ± 0.1	4.8 ± 0.0	82.6	93.6	88.9	49.3
3Ox	64.4 ± 1.2	11.0 ± 0.1	9.2 ± 0.2	1.9 ± 0.1	5.1 ± 0.2	73.1	92.2	82.9	74.8
4Ox	71.5 ± 0.3	11.1 ± 0.1	3.3 ± 0.3	1.3 ± 0.0	5.3 ± 0.5	62.8	88.0	71.5	92.1

Table 3*. Chemical composition of the original TMP, F and F-1Ox, 1 Ox, 2Ox, 3Ox, and 4Ox oxidized treatments, and mass balance results relative to the original TMP.*

*All lignin % are statistically distinct from each other with 95% confidence with the exception of TMP and F which are statistically equivalent and F-1Ox and 1Ox (TMP= F, F-1Ox = 1Ox).

4.2. Lignocellulosic nanofibril characterization

4.2.1. Chemical and morphological characterization

FTIR spectra of each LCNF sample are shown in **Figure 1a,** similar peaks were observed for all samples. The large peak at 1027 cm^{-1} corresponds to C-O-C stretching of glycosidic bonds found in cellulose [11]. The spectral band at 3335 cm^{-1} is attributed to O-H stretching in intramolecular aromatic and aliphatic hydroxyl groups on the cellulose backbone and phenolic groups in lignin [28,29]. The slight peaks at 2918 cm^{-1} are associated with symmetric and asymmetric C-H stretching of methyl and methylene groups present in cellulose and hemicellulose [11]. Peaks at 1598, 1510 and 1422 cm^{-1} are associated with aromatic ring vibrations in the lignin backbone [11,28,29]. The peak at 1367 cm^{-1} corresponds to asymmetric C-H deformation and C-O stretching in syringyl groups of lignin [29]. Peaks at 1264 cm^{-1} can be assigned to O-H deformation arising from the stretching of the phenolic C-OH group and disappear after 2, 3 and 4 PAA treatments [11]. The peaks at 1160 cm^{-1} are associated with aliphatic ether C-O stretching [20].

Conductometric titration was used to determine the charge density of LCNF samples for all oxidized samples shown in **Figure 1b**. The charge density ranged from 210.0 μmol/g for the 4Ox sample up to 357.8 μmol/g for the F-1O sample. These results are relatively low compared to LCNFs produced by TEMPO mediated oxidation of softwood TMP pulp which report a surface charge of 1600-1800 μmol/g carboxylate content [17]. This is not surprising as peracetic acid is known to work by oxidizing reducing end of cellulose chains whereas TEMPO targets carbon 6 along the whole chain [4,17,18,26]. Similar results were observed for different types of agricultural residues treated

with PAA, namely wheat straw, corn stover, reed canary grass and industrial hemp, whose carboxylate contents ranged from 105-344 μmol/g [4,30].

XRD analysis was used to explore the crystalline structure of LCNF film samples for every combination of chemical and mechanical treatment. **Figure 1c** shows that all samples displayed large peaks at 2θ angles of around 16.4° and 22.4° which correspond to (1 1 0) and (2 0 0) crystalline planes which are characteristic of cellulose I crystalline structure [11,20]. The crystallinity index for each treatment was calculated using the Segal method and ranged from 59.4% to 64.8%, with no significant difference between each treatment (α= 0.05). This result is similar to crystallinity values reported by Yang et al. of 66% for CNFs made from spruce match sticks treated by 4 PAA oxidations and mechanical fibrillation via kitchen blender with a low lignin content of 2% [31]. However, Vergara-Figueroa et al. reports a lower crystallinity index of 43% for their 32% lignin TMP-NFs produced by thorough microgrinding of radiata pine TMP and no chemical treatment [11].

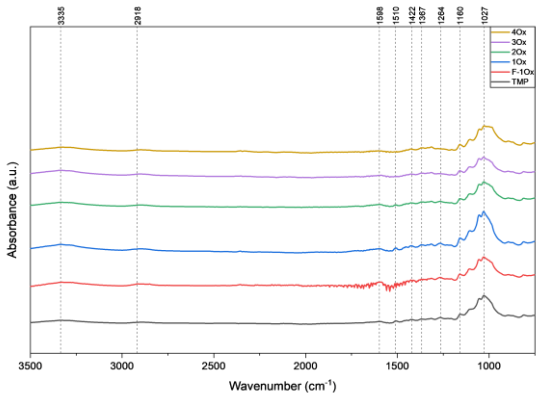

a)

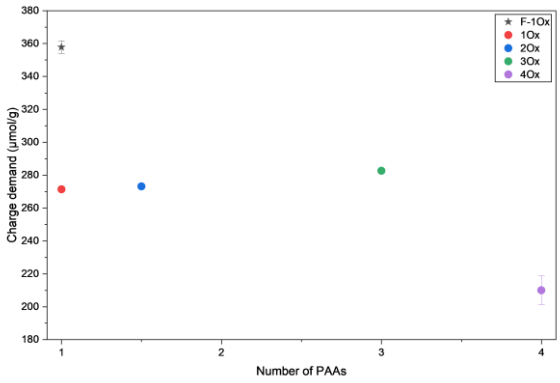

b)

c)

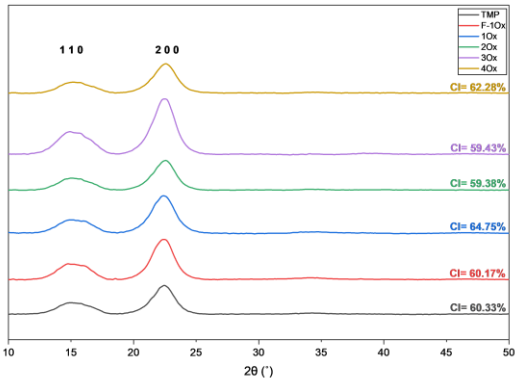

Figure 1*.a) FTIR spectra of the LCNF samples. b) Scatter plot of the charge density of the LCNF samples. c) XRD patterns of the LCNF samples.*

Based on preliminary studies in our lab (data not shown), it was found that TMP treated with 1 PAA oxidation with 5 rounds of homogenization and TMP treated with 4 PAA oxidations with 1 round of homogenization produced fibrils with nearly identical diameter size but drastically different lignin contents assuming mechanical treatment does not affect the chemical composition. These samples will be referred to as 1Ox5H and 4Ox1H respectively. To explore combination of fractionation and mechanical treatment, the F-1Ox sample was homogenized for 5 rounds to compare it to its unfractionated analog: 1Ox5H and will be referred to as F-1Ox5H.

Scanning electron microscopy analysis was performed on each of the LCNF samples and revealed a heterogeneous mixture of nano- and micro-fibrils. To quantify the degree of homogeneity in fiber diameters, the proportion of fibrils with diameters below 100 nm was calculated from the 500 measurements that were taken from each sample. The results of the SEM analysis are shown below in **Figure 2**, **Figure 3**, and **Figure 4** with size distribution curves, corresponding SEM images and the proportion of nanofibrils with diameters below 100 nm in addition to **Table 4** reporting average

diameter and standard deviation for every combination of chemical and mechanical treatment. Single factor Analysis of Variance (ANOVA) followed by a post-hoc Tukey-Kramer Multiple Comparisons test conducted at 95% confidence ($\alpha = 0.05$) showed that untreated TMP and F-TMP, along with F-1Ox and 1Ox, were not statistically different from each other, demonstrating that fractionation did not have an effect on fiber diameter. As the number of PAA oxidations increased, the percentage of fibrils with widths smaller than 100 nm increased from 28.6% for the untreated TMP up to 87.0% for the 4 PAA treated sample indicating a reduction of heterogeneity with more chemical treatment.

Mechanical treatment via homogenization reduced fiber diameter for F-1Ox from 225.8 nm to 131.9 nm after 5 passes through the microfluidizer (F-1Ox5H) (statistically different at $\alpha=0.05$). Similarly, 1Ox fibers decreased from 257.5 nm to 52.3 nm after 5 passes (1Ox5H) and % of fibers below 100 nm increased from 46.8% to 90.6% indicating successful homogenization (statistically different at $\alpha=0.05$). However, 4Ox and 4Ox1H did not demonstrate significant change in fiber diameter at $\alpha=0.05$.

In general, the type of chemical and mechanical treatment, along with separation techniques, largely impact the reported fiber sizes [1]. For example, Yang et al. treated softwood matchsticks with 4 PAA treatments and fractionated the fibers using a kitchen blender—similar to the process used in the current study to produce LCNFs [20]. However, the blended fibers were centrifuged to separate the larger fibers and the sediment was blended again to create LCNFs and reported average nanofiber diameters less than 5 nm [20]. Vergara-Figueroa et al. produced LCNF from softwood TMP fibers with widths of 35 ± 13 nm using pure mechanical microgrinding via super masscolloider and

centrifugation to separate the smaller fibers from the heterogeneous mixture [11]. Bakkari et al. (2019) demonstrated the use of microgrinding to produce LCNFs with fiber widths of 10-20 nm in combination with TEMPO mediated oxidation as a pretreatment [13]. Han et al. reported fiber diameters of 7.1- 7.6 nm after using enzymatic hydrolysis to monomerize softwood TMP, collecting the unreacted TMP fibers as LCNFs [15].

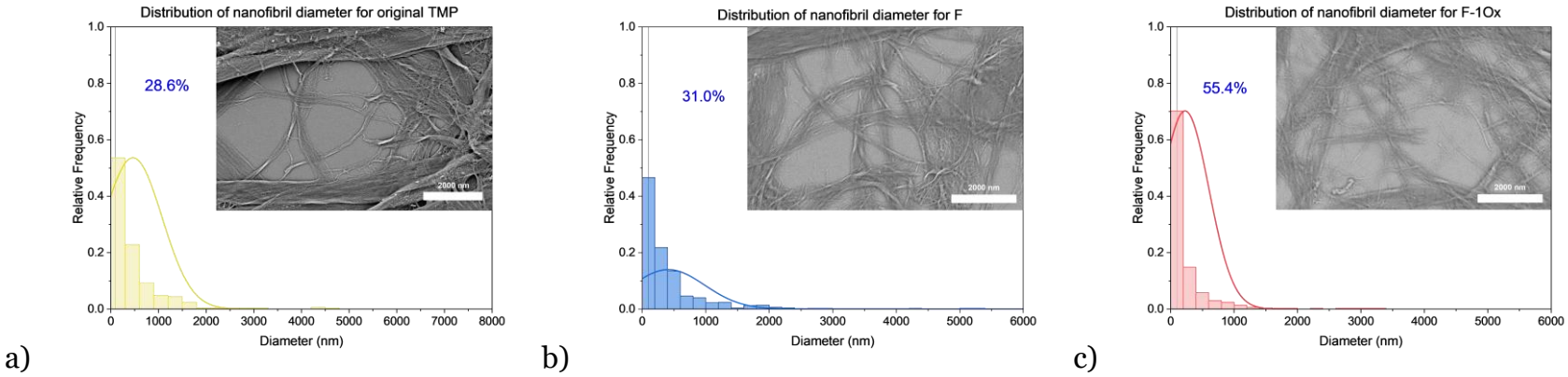

Figure 2. *Nanofibril size distribution curves, SEM images of each LCNF sample, and the corresponding proportion of nanofibrils with diameters below 100 nm for a) original TMP and fractionated samples b) F and c) F-1Ox.*

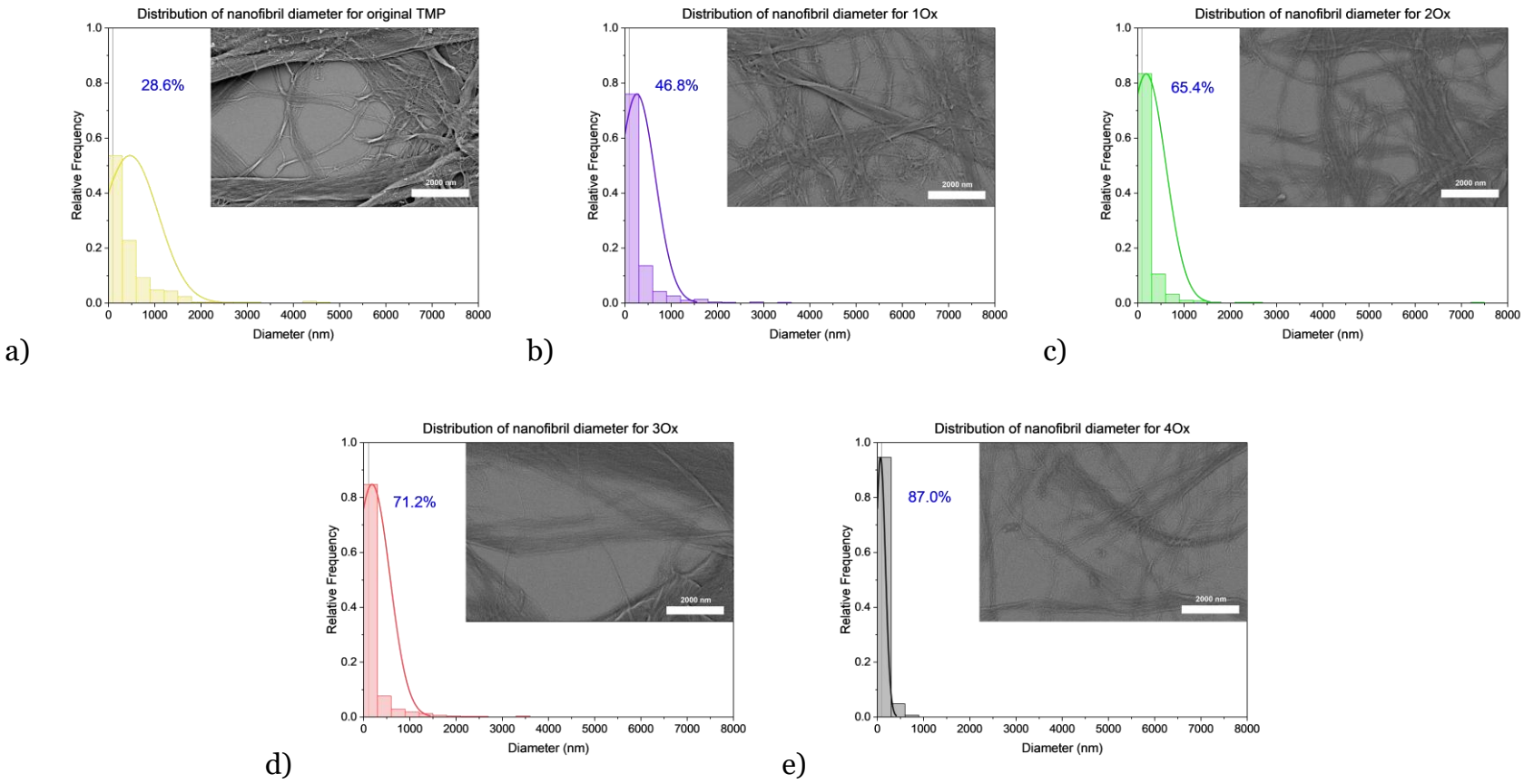

Figure 3. *Nanofibril size distribution curves, SEM images of each LCNF sample, and the corresponding proportion of nanofibrils with diameters below 100 nm for a) original TMP and oxidized samples b) 1Ox c) 2Ox d) 3Ox and e) 4Ox.*

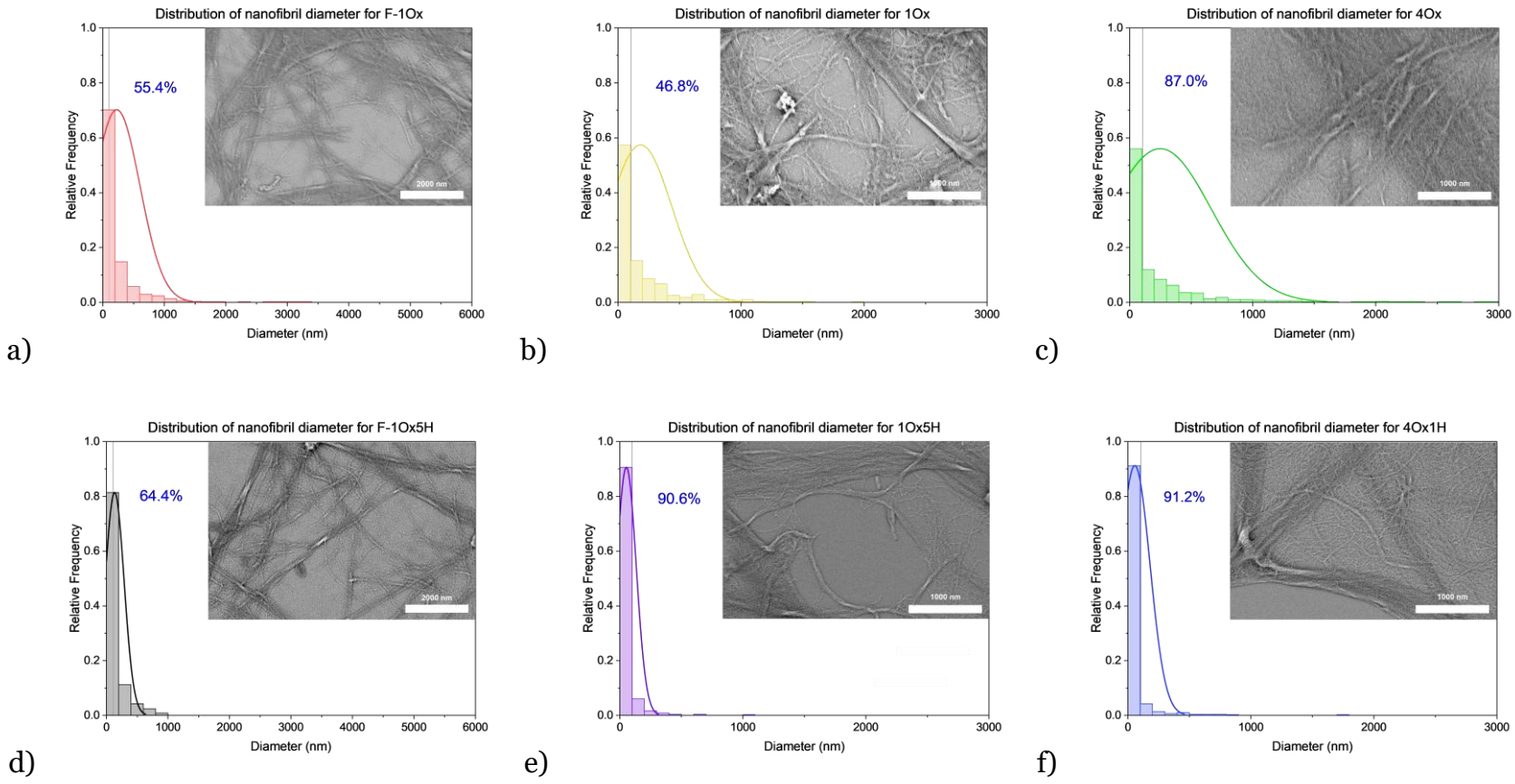

Figure 4. *Nanofibril size distribution curves, SEM images of each LCNF sample, and the corresponding proportion of nanofibrils with diameters below 100 nm for samples before mechanical treatment a) F-1Ox b) 1Ox c) 4Ox and after mechanical treatment d) F-1Ox5H e) 1Ox5H f) 4Ox1H.*

Sample	Average diameter (nm)	Standard deviation (nm)	% LCNF (<100 nm)
TMP	464.3	610.4	28.6
F	411.1	572.6	31.0
F-1Ox	225.8	337.8	55.4
1Ox	257.5	396.6	46.8
2Ox	180.3	424.2	65.4
3Ox	181.9	386.9	71.2
4Ox	69.1	104.4	87.0
F-1Ox5H	131.9	153.4	64.4
1Ox5H	52.3	79.8	90.6
4Ox1H	55.8	123.4	91.2

Table 4. *SEM analysis results for original TMP and LCNF diameters.*

Characterization of viscosity at various shear rates using a rheometer revealed that for all samples, shear thinning behavior occurred where the viscosity decreased as the shear rate increased as illustrated in **Figure 5**. Additionally, in **Figure 5b**, the viscosity profiles of 3Ox and 4Ox samples appeared to be higher than the rest, increasing as the number of PAA treatments increased. This could be attributed to a gelling behavior that is perceived in nanocellulose, which supports the conclusion that increased PAA treatments result in a greater proportion of nanosized fibers [16,32,33]. Gelling behavior due to more nanofibers is demonstrated when comparing F-1Ox and F-1Ox5H in **Figure 5c** where the homogenized sample is nearly an order of magnitude higher in viscosity than the unhomogenized sample. This is supported by preliminary data collected (data not shown) with LCNFs produced from wheat straw pulp treated

with PAA in which a majority of fibrils- from 77.4% to 97.0%- are smaller than 20 nm in diameter and report viscosities greater than 1000 Pa.s at shear rates between 0.001 and 0.01 s^{-1}. Serra-Parareda et al. also observed an increase in viscosity with more severe homogenization [16]. They attributed this behavior to the tendency of fibrils to form entangled structures where increased surface area creates more hindering interactions between fibrils, resulting in overall higher viscosity [16]. Between 1Ox5H and 4Ox1H, samples that have similar fiber diameters but very different lignin contents, 4Ox1H with lower lignin content of 3.3% exhibited a much greater viscosity than 1Ox5H, which had a higher lignin content of 23.3%.

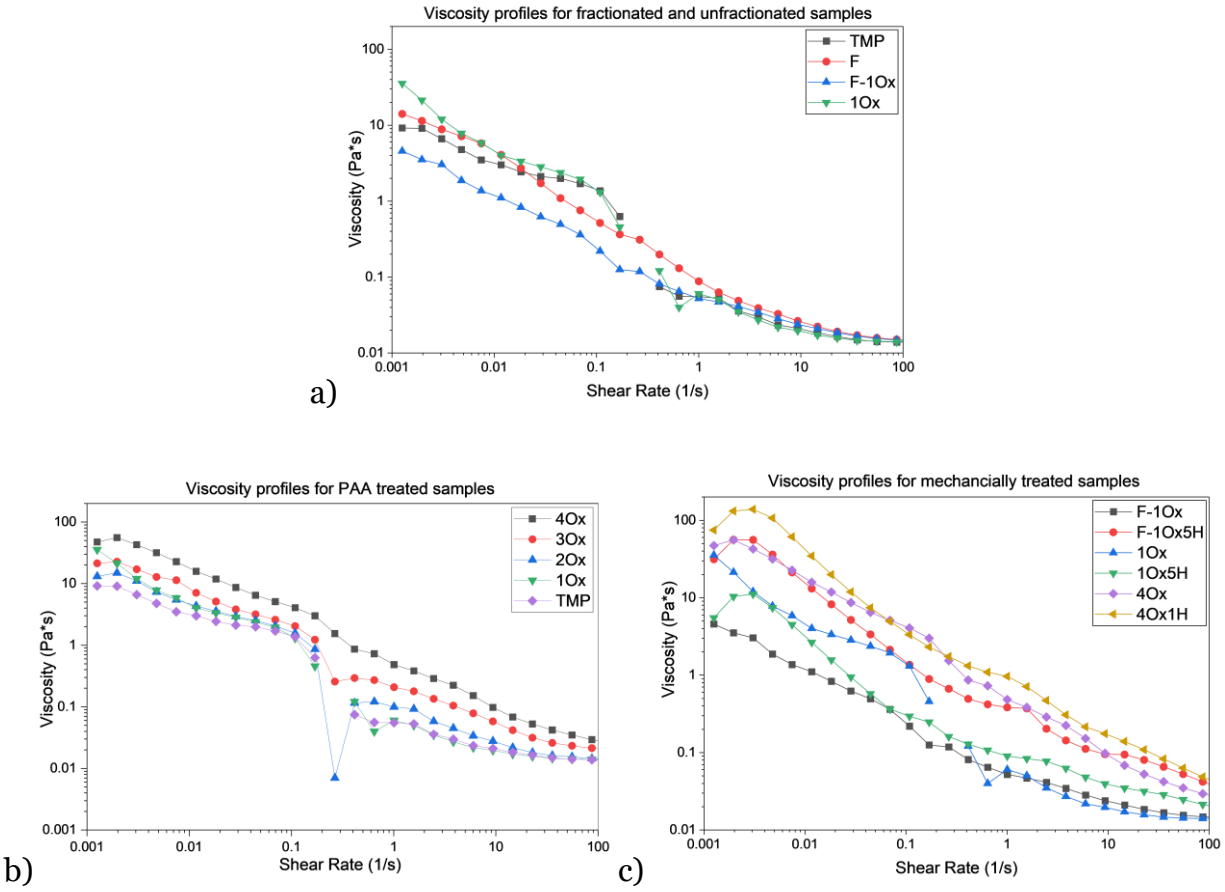

Figure 5. *Viscosity profiles for samples a) before and after fractionation b) before and after oxidation and c) before and after homogenization at 0.4% consistency.*

4.2.2. Optical properties

Optical transmittance was measured for all LCNF films from 280-800 nm wavelengths which encompasses the UV-B region (280-315 nm), UV-A region (315-400 nm) and visible region (400-800 nm) shown in **Figure 7a.** The attenuation coefficient of all film samples was calculated as a function of the absorbance standardized by thickness according to the Beer-Lambert Law and is summarized in **Table 5** below [21]. This decrease in absorbance with increased chemical treatment may have to do with the removal of lignin which has a golden-brown tint which is seen in all the films. **Figure 7b** showed that % transmittance at λ = 660 nm decreased as lignin content increased (R^2 = 61%). The highest transmittance was 82.3% for 4Ox samples with 3.3% lignin, while the lowest was 19.6% for TMP samples with 26.6% lignin. Similar results are found in CNF nanopaper films (thickness 35 μm, 2% lignin) produced by Yang et al. which demonstrated a high optical transmittance of 91% [20]. **Figure 7c** showed that % transmittance at λ = 360 nm decreased as lignin content increased, from 9.3% for 4Ox samples to 0.12% for high-lignin TMP samples (R^2 = 0.81). **Figure 7d** also showed that increasing lignin content shifted the transition to lower transmittance (5% transmittance) toward higher wavelengths, occurring between λ = 340–500 nm for all samples (R^2 = 0.69)

Samples that were treated with homogenization (F-10x5H, 10x5H and 4Ox1H) showed no observable effect of fiber diameter on attenuation coefficient when lignin content was held constant. However, comparing 1Ox5H vs. 4Ox1H (which have statistically similar fiber diameters, but different lignin contents, 24.0% and 3.3%, respectively), and holding fiber diameter constant while varying lignin content, further

supports the conclusion that increased lignin content leads to a higher attenuation coefficient. This is also demonstrated when comparing 2Ox vs. 3Ox (statistically similar fiber diameter, 16.3% and 9.2% lignin content respectively).

Sample	Attenuation coefficient @ λ=660 nm (a.u./cm)
TMP	1717.3 ± 142.1
F-1Ox	964.0 ± 140.3
1Ox	1413.9 ± 107.5
2Ox	821.7 ± 90.9
3Ox	376.5 ± 81.7
4Ox	329.0 ± 18.4
F-1Ox5H	449.2 ± 48.1
1Ox5H	2450.6 ± 153.4
4Ox1H	361.3 ± 29.8

Table 5. *Attenuation coefficients @ λ=660 nm (a.u./cm) for LCNF film samples.*

To further explore the UV-blocking properties of LCNF films, sun protection factor (SPF) was calculated using the Mansur equation and are summarized in **Table 6** [22]. SPF quantifies a materials ability to block UV-B radiation which is a known cause of sun burn and skin cancer [34]. SPF values ranged from 39.1 for 4Ox and 73.6 for TMP film samples. **Figure 6** shows a positive correlation between lignin content and SPF (R^2=82%). Lignin contains phenylpropane units and phenolic hydroxyl functional groups, which are known to protect plants from UV radiation [34,35].

Sample	SPF
TMP	73.6 ± 25.0
F-1Ox	61.6 ± 12.2
1Ox	67.2 ± 11.9
2Ox	69.1 ± 11.7
3Ox	49.7 ± 13.5
4Ox	39.1 ± 19.9
F-1Ox5H	58.9 ± 21.6
1Ox5H	72.0 ± 19.1
4Ox1H	41.6 ± 13.3

Table 6*. Sun protection factors for all LCNF film samples.*

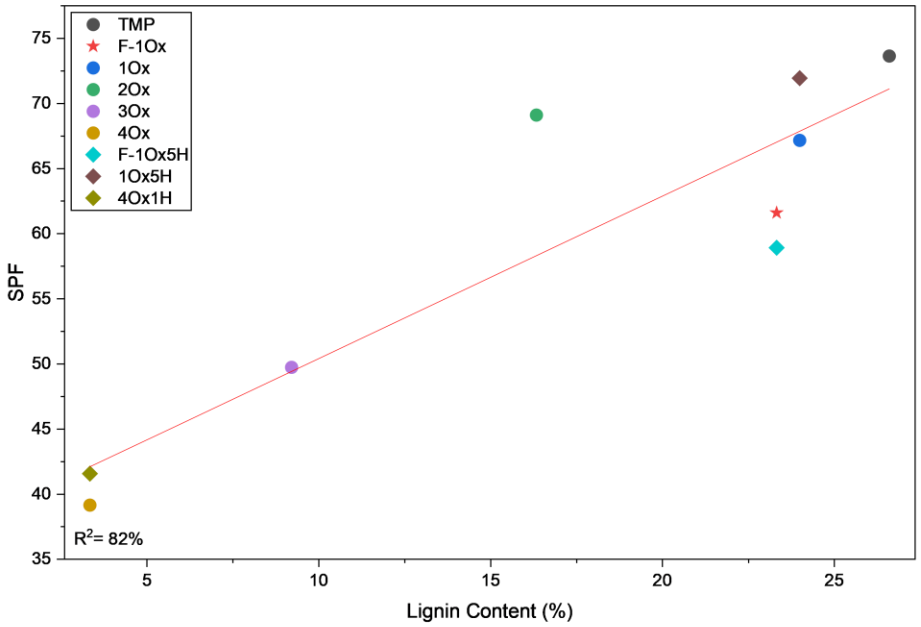

Figure 6. *Scatter plot of SPF vs. lignin content (%) with linear regression line (R^2=82%).*

Optical haze was measured within the visible spectrum (400-800 nm) for all LCNF films for each treatment and showed that optical haze decreases with increasing

PAA treatment as seen in **Figure 7e** below. LCNF films made from 4Ox LCNF sample had an average haze of 79.0% where untreated TMP LCNF films had an average of 96.4% haze. Haze is caused by the difference in refractive index at the interface between two materials, in this case cellulose and lignin, which causes light that is directed at the material to scatter [36]. This supports the finding that reduced chemical treatment, and therefore more lignin, led to increased optical haze. No observable trend on the effect of mechanical treatment on % haze was found in this study when looking at samples with the same lignin content and different fiber diameters. Not much literature exists on the optical haze for LCNF based films however, Yang et al. reported a haze value of 26% for CNF nanopapers with a lignin content of 2% [20]. Between F-1Ox and F-1Ox5H samples, which have the same lignin content but differ in fiber diameter, the haze decreased from 93.1% to 79.8%. Similarly, between 4Ox and 4Ox1H, haze decreased from 79.0% to 74.8% but this trend can be explained by a difference in thickness between each batch of films where the thicker films have increased haze.

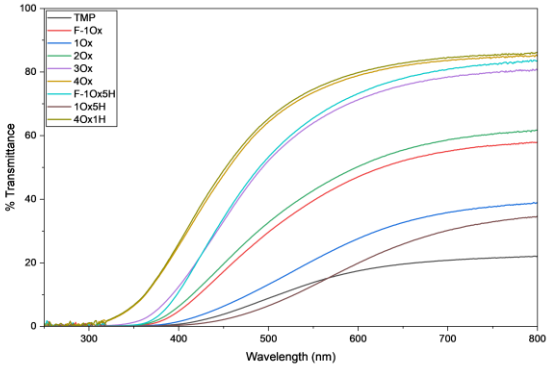

a)

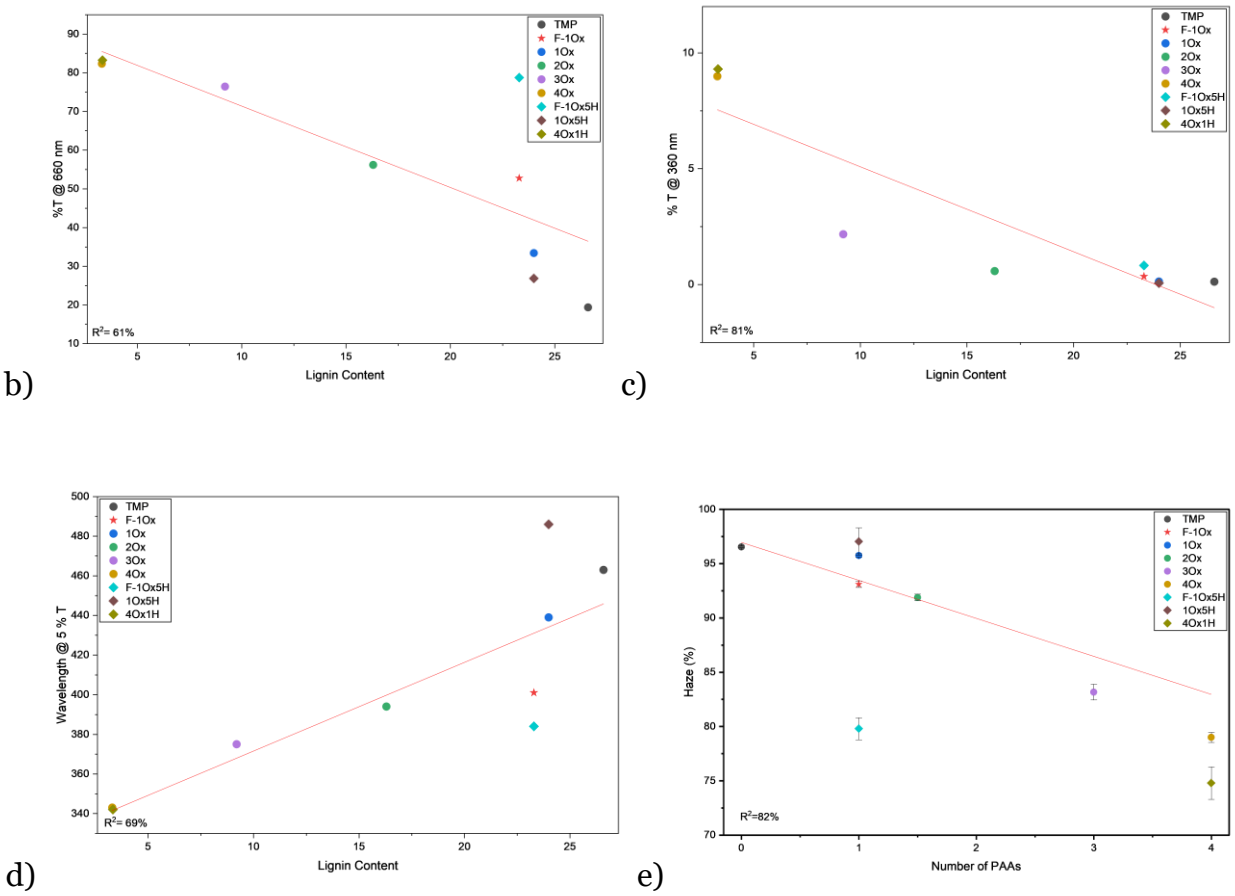

Figure 7. *a) Optical transmittance spectra of the LCNF samples b) Scatter plot of the % transmittance at λ=660 vs. lignin content c) Scatter plot of the % transmittance at λ=360 vs. lignin content d) Scatter plot of wavelength at 5% transmittance vs. lignin content e) Scatter plot of the average haze of LCNF samples against the number of PAA treatments.*

4.2.3. Thermal properties

Thermogravimetric analysis (TGA) was used to evaluate the degradation behavior and thermal stability of LCNF films of each treatment. **Figure 8** presents curves for TGA for original TMP and each treated sample (F-1Ox, 1Ox, 2Ox, 3Ox, 4Ox) along with a summary scatter plot for overall mass loss for each sample accompanied by the

summarized data in **Table 7**. For all samples, an initial mass loss of approximately 5% occurred between 50˚C and 110˚C which can be attributed to the evaporation of water from the hygroscopic films. A significant decrease in mass occurred between 200˚C and 350˚C where around 40-50% of mass was lost associated with the pyrolysis of cellulose, hemicellulose and lignin [37]. Beyond 350˚C additional mass loss of about 10-15% occurred be the degradation of aromatic lignin [38]. Residual mass ranged from 24.2% for the 4Ox samples to 29.2% for F-1Ox. Findings within our research group report similar thermal degradation behavior of LCNFs produces using PAA oxidation treatment of wheat straw pulp [4]. Pascoli et al. and Sidhu et al. reported a similar loss of up to 10% mass due to the evaporation of water from the materials, rapid degradation stage between 200˚C to 400˚C due to the loss of cellulose, hemicellulose and lignin and a final gradual decrease in mass with the charring of aromatic lignin [4,39]. The results of TGA demonstrated overall similar thermal behavior between each level of chemical treatment showing that chemical treatment did not influence the thermal stability of the LCNFs.

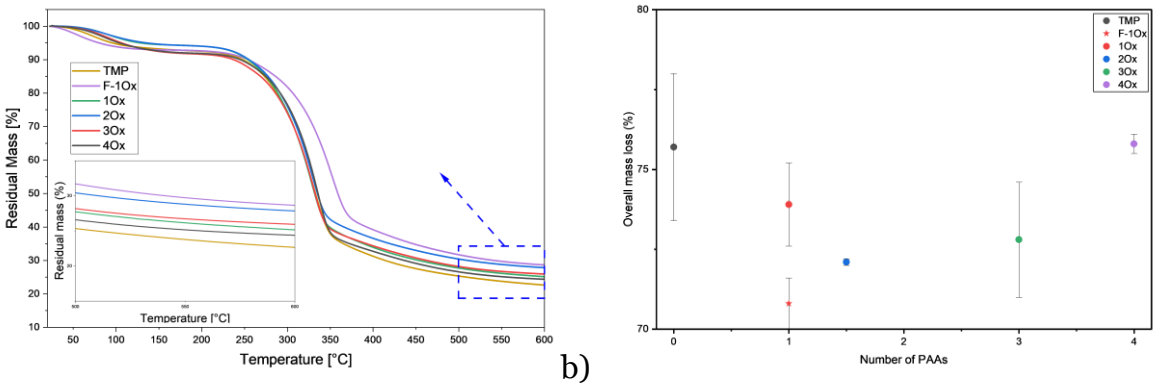

Figure 8. *a) TGA curve; TGA curve from 500°C to 600°C (bottom left) b) Scatter plot showing the relationship between the thermal mass loss percentage and the number of PAA treatments.*

Sample	Peak Temperature (˚C)	Overall mass loss (%)	Residual mass at 110˚C (%)	Residual mass at peak temperature (%)	Residual mass at 600˚C (%)
TMP	329.4 ± 3.9	75.7 ± 2.3	94.3 ± 0.1	53.1 ± 1.6	24.3 ± 2.3
F-1Ox	344.4 ± 1.2	70.8 ± 0.8	93.8 ± 0.6	56.4 ± 1.2	29.2 ± 0.8
1Ox	327.0 ± 4.9	73.9 ± 1.3	95.1 ± 1.1	53.6 ± 0.8	26.1 ± 1.3
2Ox	332.4 ± 1.1	72.1 ± 0.1	95.3 ± 1.1	54.0 ± 1.0	27.9 ± 0.1
3Ox	332.3 ± 0.9	72.8 ± 1.8	94.5 ± 0.1	52.5 ± 1.1	27.2 ± 1.8
4Ox	338.9 ± 0.5	75.8 ±0.3	94.4 ± 0.1	49.1 ± 0.0	24.2 ± 0.3

Table 7. *TGA summary characteristics for all LCNF samples.*

4.2.4. Wetting behavior and surface free energy

Drop shape analysis was used to evaluate the water contact angle (WCA) and surface free energy of all film samples including original TMP, F, all Ox samples and subsequent homogenized LCNFs summarized in **Table 8**. **Figure 9** showed that WCA decreased as fiber diameter increased. Among the TMP, 1Ox, 2Ox, 3Ox, and 4Ox samples, WCA showed a strong negative linear correlation with fiber diameter (R^2 = 77%), indicating that increased PAA oxidation reduced fiber diameter and increased WCA. Comparing samples before and after homogenization showed that the contact angle increased from 66.8° for F-1Ox films to 81.5° for F-1Ox5H films. A similar but smaller increase was observed for the 1Ox and 1Ox5H samples, indicating that films with similar lignin contents but smaller fiber diameters exhibited higher WCA and reduced hydrophilicity. In contrast, the 4Ox and 4Ox1H films showed no change in WCA, consistent with their similar lignin content and fiber diameter. These results suggested that the increase in WCA with decreasing fiber diameter was related to

increased surface roughness, which enhanced the intrinsic wettability behavior of the material. These WCA results are smaller than those of Han et al. where LCNFs recovered as a byproduct of sugar production via enzymatic hydrolysis of TMP fibers had average diameters of 7.1-7.6 nm resulted in high WCAs of 80.4-82.8°[15].

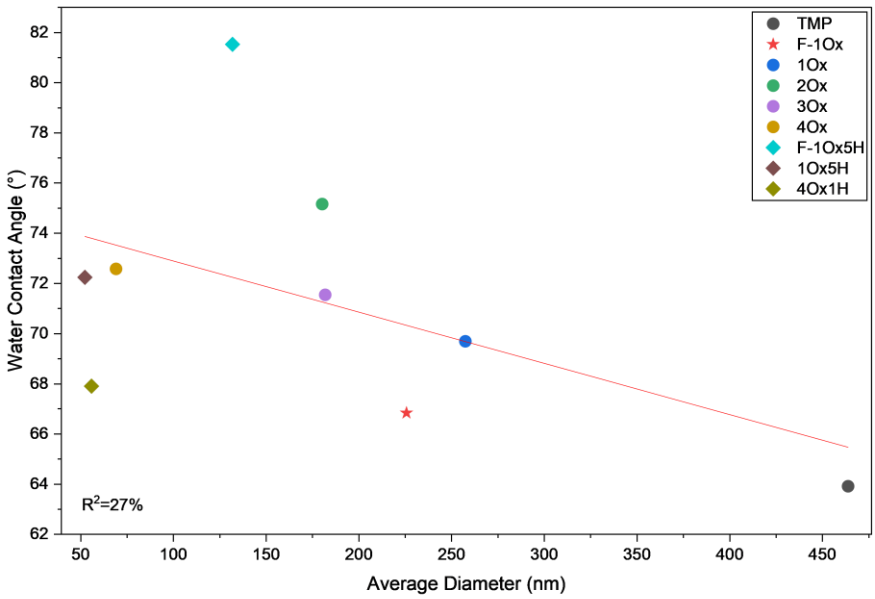

Figure 9*. Scatter plot showing relationship between fiber diameter and water contact angle for all LCNF film samples.*

To explore the effect of lignin content on water contact angle (WCA), we compared the 1Ox5H and 4Ox1H samples, which have similar fiber diameters but different lignin contents of 24.0% and 3.3%, respectively. We observed that the sample with the higher lignin content exhibited a higher WCA than the sample with the lower lignin content. The 2Ox (16.3% lignin) and 3Ox (9.2% lignin) films demonstrated a similar trend, as they also possessed comparable fiber diameters while the sample with the higher lignin content showed a greater WCA. These results indicate that samples with similar fiber diameters, but different lignin contents can be produced either

through combinations of varying chemical and mechanical treatments (1Ox5H vs. 4Ox1H) or through variations in chemical treatment alone (2Ox vs. 3Ox), depending on the desired material performance. This also reveals that increasing the severity of chemical treatments has competing effects on surface wettability. More chemical treatment reduces fiber diameter which increased the water contact angle but removes lignin in the process which leads decreased contact angle. Overall, fiber diameter appears to have a greater effect on surface wettability than lignin content. Work within our research group with PAA oxidized wheat straw demonstrated an increased contact angle from 80.2˚ to 92.3˚ with increasing lignin content while the fiber diameter remained the same [39]. In Vergara-Figueroa et al., purely mechanically treated TMP-NF films (32.25% lignin) exhibited water contact angles ranging from 71.0° to 84.6°, compared to pure CNF films (~0% lignin), which exhibited water contact angles ranging from 56.8° to 61.5°[11].

The surface free energy of the LCNF film samples was calculated using the Owens, Wendt, Rabel and Kaelble (OWRK) method, which involves collecting contact angle data for water and diiodomethane and calculating the polar and disperse components of surface free energy [40]. The polar component accounts for the surface interactions of dipoles and hydrogen bonding and the disperse component accounts for London dispersion forces [40]. The total surface free energy ranged from 35.9 mJ/m² for F-1Ox5H films to 48.7 mJ/m² for original TMP films.

Sample	WCA (˚)	DCA (˚)	Disperse (mJ/m²)	Polar (mJ/m²)	SFE (mJ/m²)
Original TMP	63.9 ± 2.0	43.8 ± 2.0	37.7	11.1	48.7
F-1Ox	66.8 ± 1.9	54.9 ± 2.0	31.5	11.8	43.3
1Ox	69.7 ± 2.0	48.9 ± 2.0	34.9	9.0	43.9
2Ox	75.2 ± 2.0	49.4 ± 2.0	34.6	6.5	41.2
3Ox	71.5 ± 2.0	50.3 ± 2.0	34.1	8.4	42.5
4Ox	72.6 ± 1.9	51.7 ±2.0	33.3	8.1	41.4
F-1Ox5H	81.5 ± 2.0	55.6 ± 2.0	31.1	4.9	35.9
1Ox5H	72.2 ± 2.0	56.6 ± 2.0	30.5	9.3	39.8
4Ox1H	67.9 ± 2.0	57.3 ± 2.0	30.2	11.7	41.9

Table 8. *Drop shape analysis summary characteristics for the LCNF film samples.*

*All WCA (˚) are statistically distinct with 95% confidence with the exception of 3Ox and 4Ox which are statically equivalent (3Ox= 4Ox).

4.2.5. Mechanical properties

Tensile testing was conducted on all Ox LCNF film samples (i.e. F-1Ox, 1-4Ox, F-1OxH, 1Ox5H and 4Ox1H) to quantify their mechanical properties, summarized in **Table 9**. From 1Ox to 4Ox, the elastic modulus increased from 4.4 GPa to 6.9 GPa and the ultimate tensile strength also increased from 46.1 MPa to 95.4 MPa. With increasing chemical treatment, the lignin content and fiber diameter decreased, resulting in increased elastic modulus and ultimate tensile strength. An inverse relationship

between lignin content and ultimate tensile strength was also observed by Sidhu with LCNF films with varying lignin contents produced from wheat straw [39].

Among the samples before homogenization (F-1Ox, 1Ox, and 4Ox) and after homogenization (F-1Ox5H, 1Ox5H, and 4Ox1H), films made from LCNFs with identical lignin contents, but different fiber diameters exhibited increased elastic modulus and ultimate tensile strength as fiber diameter decreased. F-1Ox (average fiber diameter = 225.3 ± 337.8 nm) had an elastic modulus of 5.9 GPa and an ultimate tensile strength of 49.6 MPa, whereas its homogenized counterpart, F-1Ox5H (average fiber diameter = 131.9 ± 153.4 nm), exhibited higher values, with an elastic modulus of 7.8 GPa and an ultimate tensile strength of 82.1 MPa. Similar trends in mechanical properties were observed between 1Ox and 1Ox5H but not between 4Ox and 4Ox1H, as there were no statistically significant differences in fiber diameter for these samples.

The role of lignin content independent of fiber diameter can be studied by comparing 1Ox5H with 4Ox1H and 2Ox with 3Ox, as each pair has similar fiber diameters but different lignin contents. In doing so, it is observed that samples with similar diameters but different lignin contents show no significant difference in elastic modulus or ultimate tensile strength. LCNF films for 1Ox5H (24.0% lignin) had an elastic modulus of 7.1 GPa and an ultimate tensile strength of 68.8 MPa, which are comparable to the values of 7.3 GPa and 82.1 MPa, respectively, for 4Ox1H (3.3% lignin). Similarly, the elastic modulus and ultimate tensile strength for 2Ox (16.3% lignin) were 5.1 GPa and 55.5 MPa, and for 3Ox (9.2% lignin) were 5.7 GPa and 65.2 MPa.

Fiber diameter strongly influenced the mechanical properties of LCNF films, as smaller fibers increased specific surface area and enhanced interfibrillar bonding, resulting in stiffer and stronger films [4,39]. Hemicellulose also contributed to improved mechanical performance, as the high recovery rates observed after PAA oxidation promoted fibril dispersion, strengthened the fiber network, and improved stress transfer during failure [20,31,41]. Together, the presence of hemicellulose and the reduced fiber diameter enhanced fiber–fiber bonding, leading to materials with greater stiffness and strength that showed potential for packaging and composite applications [20,31,41].

Sidhu has shown that increasing lignin from 2.6% to 7.7% increased peak elongation from 0.8% to 3.2% for wheat straw LCNF film samples [39]. In this study, peak elongation, also known as strain at break, ranged from 1.1-3.3% across all the samples and was not consistent with Sidhu's findings as no trend was observed due to the lack of statistical differences among the samples [39].

	Elastic Modulus (GPa)	Ultimate Tensile Strength (MPa)	Peak Elongation (%)
F-1Ox	5.8 ± 0.2	49.6 ± 0.7	1.1 ± 0.0
1Ox	4.4 ± 0.3	46.1 ± 3.6	1.5 ± 0.2
2Ox	5.1 ± 0.3	55.5 ± 21.3	1.7 ± 0.7
3Ox	5.7 ± 0.2	65.2 ± 0.2	2.1 ± 0.9
4Ox	6.9 ± 0.1	95.4 ± 9.6	3.3 ± 1.0
F-1Ox5H	7.8 ± 0.1	82.1 ± 1.1	1.8 ± 0.2
1Ox5H	7.1 ± 0.2	66.8 ± 2.6	1.7 ± 0.1
4Ox1H	7.3 ± 0.2	82.1 ± 1.1	2.2 ± 0.3

***Table 9**. Summary of mechanical properties for the LCNF film samples.*

The results of this study demonstrate that the physical and chemical properties of LCNFs can be tailored through different combinations of chemical and mechanical treatments. Overall, increased severity of the chemical treatment decreased overall mass yields due to lignin and hemicellulose loss. Lignin loss led to increased visible light transmittance and decreased sun protection factor and haze. Increased severity of the chemical treatment also decreased the average fiber diameter of the LCNFs accompanied by increased homogeneity, viscosity, surface wettability, elastic modulus and ultimate tensile strength. Similarly, increased severity of the mechanical treatment

decreased fiber diameters and increased homogeneity, viscosity, surface wettability, elastic modulus, and ultimate tensile strength without altering the chemical composition of the LCNFs.

There are several treatment pathways you can take to produce LCNFs with specific properties. LCNFs with lower lignin contents can be achieved by increasing severity of chemical treatment, i,e., the number of PAA oxidations, resulting in fibers with smaller average diameters (1Ox vs. 2Ox vs. 3Ox vs. 4Ox). Smaller fiber diameters can also be achieved without changing the chemical composition by using more severe mechanical treatments (F-1Ox5H, 1Ox5H, 4Ox1H). 2Ox and 3Ox samples demonstrate that you can produce similar fiber diameters with different lignin contents with chemical treatment alone. When multiple treatment methods produce materials with similar characteristics and performance, selecting the most suitable process cannot be based on material properties alone. Therefore, a techno-economic analysis (TEA) is necessary to evaluate the economic feasibility and overall process efficiency of the different treatment strategies.

4.3. Techno-economic analysis

The breakdown of total capital investment (TCI) is shown in **Table 10**. The most expensive equipment in both scenarios was the microfluidizer, particularly in the 1Ox5H process which requires over 7 times as many microfluidizers as the 4Ox1H scenario due to its higher yield and greater number of passes. However, the 4Ox1H scenario requires a much larger wastewater treatment plant due to its increased usage of PAA in the oxidation step. Despite this, the 1Ox5H process had a higher TCI than the 4Ox1H process.

	10x5H cost	40x1H cost
Purchased equipment	$48,500,000	$10,000,000
Equipment installation	$18,900,000	$3,900,000
Instrumentations and control	$12,600,000	$2,600,000
Piping	$15,000,000	$3,100,000
Electrical System and buildings	$18,900,000	$3,900,000
Yard improvements	$5,800,000	$1,200,000
Service facilities	$26,700,000	$5,500,00
Wastewater treatment	$28,000,000	$64,300,000
Total direct costs (TDC)	**$174,500,000**	**$94,400,000**
Proratable expenses	$17,400,000	$9,400,000
Field expenses	$17,400,000	$9,400,000
Office construction	$34,900,000	$18,900,000
Project contingency	$17,400,000	$9,400,000
Other costs (start-up, permits, etc.)	$17,400,000	$9,400,000
Total indirect costs (TIC)	**$104,700,000**	**$56,600,000**
Fixed capital investment	**$279,100,000**	**$151,000,000**
Working capital	$14,000,000	$7,600,000
Total capital investment (TCI)	**$293,100,000**	**$158,600,000**

Table 10. *Breakdown of Total Capital Investment (TCI).*

The total operating cost breakdown is shown in **Table 11**. Hydrogen peroxide and acetic acid, both used in the PAA production step, contributed to the majority of the chemical variable costs especially in the 40x1H process as it uses 4 times as much as the 10x5H process. Natural gas cost was also 4 times higher for the 40x1H process compared to the 10x5H process due to the increased number of reactions that require gas to heat them to reaction temperature. However, the 10x5H process had a

significantly higher grid electricity cost of ~$60 million compared to ~$8 million for the 4Ox1H process. This is attributed to the increased energy demand to power the microfluidizers, in which the 1Ox5H process has over 7 times as many as the 4Ox1H process. Overall, the 4Ox1H scenario has a greater total variable cost, and subsequent total operating costs, than the 1Ox5H scenario.

	Price	**1Ox5H cost ($/year)**	**4Ox1H cost ($/year)**
Feedstock (TMP)	$440/tonne	15,400,000	15,400,000
NaOH	$352.42/tonne	1,200,000	4,900,000
H_2O_2	$702/tonne	9,800,000	39,300,000
Acetic acid	$750/tonne	22,000,000	88,100,000
H_2SO_4	$88/tonne	100,000	400,000
Natural gas	$3.02/MMBtu	628,000	2,500,000
Grid electricity	$0.075/kWh	59,800,000	7,800,000
Total variable costs		**109,000,000**	**158,400,000**
Operating labor salaries	Total of 4 employees/ area	4,000,000	5,000,000
Operating supervision	15% of operating labor	600,000	750,000
Labor burden	90% of total salaries	3,600,000	4,500,000
Maintenance	10% FCI	27,900,00	15,100,000
Laboratory charges	15% of operating labor	600,000	750,000
Operating supplies	1% FCI	2,800,000	1,500,000
Property insurance	1% FCI	2,800,000	1,500,000
Total fixed costs		**42,300,000**	**29,100,000**
Total operating costs		**151,300,000**	**187,500,000**

Table 11. *Breakdown of Total Operating Costs (TOC).*

A discounted cash flow analysis was performed using the estimated capital and operating costs over a 10-year financing period in which minimum product selling price (MPSP) was calculated for each process at various discount rates, summarized in **Table 12**. The MPSP of 1Ox5H LCNFs ranged from $5.57/kg (oven dry) at a break-even 0% discount rate to $6.50/kg at a favorable profit margin with a 20% discount rate. MPSP of 4Ox1H were comparatively higher, ranging from $9.47/kg at a 0% discount rate to $10.26/kg at a 20% discount rate. Pascoli reports lower MPSP for LCNFs made of wheat straw, ranging from $3.83/kg for 0% discount rate to $4.60/kg with a 15% discount rate (For comparison, the MPSP for the 4Ox1H at a 15% discount rate was found to be $6.23/kg). The lower MPSP for Pascoli can be attributed to the use of an agricultural waste as a low-cost feedstock, as well as the application of lower-severity chemical and mechanical treatments, which reduce operating and capital costs [19]. Market data surrounding nanocellulose is limited as the industry is still small but some sources list prices for nanocellulose from $13-$35,000/kg depending on the product (fiber size, surface modification, chemical composition etc.) [42]. The results of this study show that it is possible to produce LCNF with versatile characteristics at significantly lower prices than currently available purchasing options.

IRR	10x5H price ($/kg product)	40x1H price ($/kg product)
0%	5.57	9.47
7%	5.85	9.71
15%	6.23	10.03
20%	6.50	10.26

Table 12. *MPSPs for each process at various discount rates.*

5. Conclusions

This study elucidates a novel method for producing lignocellulosic nanofibrils (LCNFs) from thermomechanically pulped (TMP) softwood fibers using various combinations of chemical treatment, including alkaline peroxide fractionation and peracetic acid (PAA) oxidation, followed by mechanical homogenization. Alkaline peroxide fractionation had no observable effect on the chemical composition of the TMP fibers due to the low reaction temperature (87 °C). Increasing the severity of the chemical treatment, specifically by application of multiple PAA oxidation pretreatments, resulted in lower lignin and hemicellulose contents, reduced overall mass yields, and the isolation of nanofibrils with a wide range of chemical and physical properties. These properties include small fibril diameters, increased fibril diameter homogeneity, viscosity, and higher elastic modulus and ultimate tensile strength. More severe chemical treatment also decreased visible light absorbance, sun protection factor, and haze. Interestingly, the effects of increasing chemical treatment severity on surface

wettability were conflicting, with reduced fiber diameter leading to lower hydrophilicity and reduced lignin content leading to higher hydrophilicity.

Functional groups, surface charge density, crystallinity and thermal properties remained unchanged with increasing chemical treatment severity. Increased mechanical treatment severity through homogenization produced LCNFs with smaller average diameters and greater uniformity while maintaining their chemical composition. Reduced fibril diameters resulted in increased viscosity, water contact angle, stiffness, and strength properties. Overall, different combinations of chemical and mechanical treatments enabled the production of lignocellulosic nanofibrils with tunable chemical, physical, and optical properties from thermomechanically pulped softwood fibers.

Discounted cash flow analysis revealed that between commercial scale processes for 1Ox5H (most severe mechanical treatment) and 4Ox1H (most severe chemical treatment), 1Ox5H LCNFs could be produced at a lower MPSP. 1Ox5H had an MPSP of $5.58/kg at discount rate of 0% compared to 4Ox1H LCNFs at $9.47/kg at the same discount rate. These prices are competitive with current purchasable cellulose nanofibrils, which demonstrates the commercial feasibility of this tunable process. Furthermore, the results of this study lay the framework for future studies into the commercial scale production of LCNFs from alterative feedstocks. First, the feasibility of producing LCNFs from a given feedstock must be demonstrated through the development and evaluation of suitable chemical and/or mechanical treatments. Next, the process should be sufficiently understood and optimized to enable tuning of LCNFs properties a range of end-use applications. Finally, the economic viability of the process must be established through techno-economic assessment at commercial scale. By

following this road map, LCNF production can progress beyond laboratory-scale research toward pilot-scale demonstration and eventual industrial implementation, enabling the sustainable, high-volume, and cost-effective manufacture of these materials for diverse applications.

6. Future work

The discoveries in this study open several avenues for further LCNF research. Softwood sawdust could undergo similar chemical and mechanical treatments to evaluate its potential as an LCNF feedstock more relevant to the forest products industry. Additionally, the post-PAA washing step could be optimized to reduce water demand and improve process sustainability.

This study also highlights opportunities for further analysis. Viscosity changes were assessed qualitatively through visual comparison of viscosity profiles over the shear-rate range. Rheological behavior could be better quantified using parameters such as the consistency index (k) and flow behavior index (n). In addition, nanofibril size distributions were described using normal distribution parameters for consistency with prior literature, despite the histograms more closely resembling gamma distributions defined by shape and scale parameters. Accordingly, Generalized Linear Models (GLMs) may be more appropriate than ANOVA for future statistical analyses.

7. References

1. Dufresne, A. Nanocellulose: a new ageless bionanomaterial. *Mater. Today* **16**, 220–227 (2013).
2. Cellulose - an overview | ScienceDirect Topics. https://www.sciencedirect.com/topics/biochemistry-genetics-and-molecular-biology/cellulose.
3. A Robust Process to Produce Lignocellulosic Nanofibers from Corn Stover, Reed Canary Grass, and Industrial Hemp. https://www.mdpi.com/2073-4360/15/4/937.
4. Pascoli, D. U., Dichiara, A., Roumeli, E., Gustafson, R. & Bura, R. Lignocellulosic nanomaterials production from wheat straw via peracetic acid pretreatment and their application in plastic composites. *Carbohydr. Polym.* **295**, 119857 (2022).
5. Liu, W. *et al.* Sustainable preparation of lignocellulosic nanofibrils and cellulose nanopaper from poplar sawdust. *J. Clean. Prod.* **384**, 135582 (2023).
6. Mboowa, D. A review of the traditional pulping methods and the recent improvements in the pulping processes. *Biomass Convers. Biorefinery* **14**, 1–12 (2024).
7. Mezencevova, A., Garas, V., Nanko, H. & Kurtis, K. E. Influence of Thermomechanical Pulp Fiber Compositions on Internal Curing of Cementitious Materials. *J. Mater. Civ. Eng.* **24**, 970–975 (2012).
8. Cascade Pacific Pulp – High Grade Market Pulp from the Pacific Northwest. https://cascadepulp.com/.

9. NORPAC - Washington State Department of Ecology. https://ecology.wa.gov/regulations-permits/permits-certifications/industrial-facilities-permits/norpac.
10. Pulp & paper | Oregon Forest Industry Directory. https://orforestdirectory.com/categories/products-produced/pulp-paper.
11. Vergara-Figueroa, J. *et al.* Development of Thin Films from Thermomechanical Pulp Nanofibers of Radiata Pine (Pinus radiata D. Don) for Applications in Bio-Based Nanocomposites. *Fibers* **11**, 1 (2022).
12. Osong, S. H., Norgren, S. & Engstrand, P. An approach to produce nano-ligno-cellulose from mechanical pulp fine materials. *Nord. Pulp Pap. Res. J.* **28**, 472–479 (2013).
13. Bakkari, M. E., Bindiganavile, V., Goncalves, J. & Boluk, Y. Preparation of cellulose nanofibers by TEMPO-oxidation of bleached chemi-thermomechanical pulp for cement applications. *Carbohydr. Polym.* **203**, 238–245 (2019).
14. Jiang, J. *et al.* Acidic deep eutectic solvent assisted isolation of lignin containing nanocellulose from thermomechanical pulp. *Carbohydr. Polym.* **247**, 116727 (2020).
15. Han, X. *et al.* Potential To Produce Sugars and Lignin-Containing Cellulose Nanofibrils from Enzymatically Hydrolyzed Chemi-Thermomechanical Pulps. *ACS Sustain. Chem. Eng.* **8**, 14955–14963 (2020).
16. Serra-Parareda, F. *et al.* Correlation between rheological measurements and morphological features of lignocellulosic micro/nanofibers from different softwood sources. *Int. J. Biol. Macromol.* **187**, 789–799 (2021).

17. Jiang, J. *et al.* Influence of Chemical and Enzymatic TEMPO-Mediated Oxidation on Chemical Structure and Nanofibrillation of Lignocellulose. *ACS Sustain. Chem. Eng.* **8**, 14198–14206 (2020).
18. Patankar, Saurabh. C. & Renneckar, S. Greener synthesis of nanofibrillated cellulose using magnetically separable TEMPO nanocatalyst. *Green Chem* **19**, 4792–4797 (2017).
19. Pascoli, D. U. Nanocellulose production from low-cost agricultural residues: process development, economic assessment, and process robustness.
20. Yang, X., Reid, M. S., Olsén, P. & Berglund, L. A. Eco-Friendly Cellulose Nanofibrils Designed by Nature: Effects from Preserving Native State. *ACS Nano* **14**, 724–735 (2020).
21. Beer-Lambert Law | Transmittance & Absorbance. https://www.edinst.com/resource/the-beer-lambert-law/ (2021).
22. Mbanga, L. *et al.* Determination of Sun Protection Factor (SPF) of Some Body Creams and Lotions Marketed in Kinshasa by Ultraviolet Spectrophotometry.
23. ASTM D1003-21 Standard Test Method for Haze and Luminous Transmittance of Transparent Plastics. https://compass.astm.org/content-access?contentCode=ASTM%7CD1003-21%7Cen-US.
24. Alvarez-Vasco, C. & Zhang, X. Alkaline hydrogen peroxide pretreatment of softwood: Hemicellulose degradation pathways. *Bioresour. Technol.* **150**, 321–327 (2013).
25. Albrecht, J. S. An investigation of the physical-chemical mechanism of selective delignification of wood with peracetic acid.
26. Ronning, D. C. Peroxyacetic Acid Delignification of Wood and Bark from Ponderosa Pine (Pinus ponderosa).

27. *The Chemistry of Solid Wood*. vol. 207 (American Chemical Society, Washington, DC, 1984).

28. Espinosa, E., Domínguez-Robles, J., Sánchez, R., Tarrés, Q. & Rodríguez, A. The effect of pre-treatment on the production of lignocellulosic nanofibers and their application as a reinforcing agent in paper. *Cellulose* **24**, 2605–2618 (2017).

30. Pascoli, D. U., Dichiara, A., Gustafson, R. & Bura, R. A Robust Process to Produce Lignocellulosic Nanofibers from Corn Stover, Reed Canary Grass, and Industrial Hemp. *Polymers* **15**, 937 (2023).

31. Yang, X., Berthold, F. & Berglund, L. A. Preserving Cellulose Structure: Delignified Wood Fibers for Paper Structures of High Strength and Transparency. *Biomacromolecules* **19**, 3020–3029 (2018).

32. Carneiro Pessan, C., Silva Bernardes, J., Bettini, S. H. P. & Leite, E. R. Oxidized cellulose nanofibers from sugarcane bagasse obtained by microfluidization: Morphology and rheological behavior. *Carbohydr. Polym.* **304**, 120505 (2023).

33. Xu, J., Wang, P., Yuan, B. & Zhang, H. Rheology of cellulose nanocrystal and nanofibril suspensions. *Carbohydr. Polym.* **324**, 121527 (2024).

34. Edmundson, D. D., Gustafson, R. R. & Dichiara, A. B. Sonochemical synthesis of lignin nanoparticles and their applications in poly (vinyl) alcohol composites. *Int. J. Biol. Macromol.* **254**, 127487 (2024).

35. Qiu, X., Li, Y., Qian, Y., Wang, J. & Zhu, S. Long-Acting and Safe Sunscreens with Ultrahigh Sun Protection Factor via Natural Lignin Encapsulation and Synergy. *ACS Appl. Bio Mater.* **1**, 1276–1285 (2018).

36. Li, Y., Fu, Q., Yu, S., Yan, M. & Berglund, L. Optically Transparent Wood from a Nanoporous Cellulosic Template: Combining Functional and Structural Performance. *Biomacromolecules* **17**, 1358–1364 (2016).
37. Yang, H., Yan, R., Chen, H., Lee, D. H. & Zheng, C. Characteristics of hemicellulose, cellulose and lignin pyrolysis. *Fuel* **86**, 1781–1788 (2007).
38. (PDF) The Impact of Biomass Composition Variability on the Char Features and Yields Resulted through Thermochemical Processes. *ResearchGate* https://doi.org/10.3390/polym16162334 (2025) doi:10.3390/polym16162334.
39. Sidhu, A. Novel production of lignocellulosic nanofibrils with diverse physical and chemical characteristics from wheat straw.
40. OWRK method – Owens, Wendt, Rabel and Kaelble model. https://www.biolinscientific.com/blog/owrk-method-owens-wendt-rabel-and-kaelble-model.
41. Yang, X., Berthold, F. & Berglund, L. A. High-Density Molded Cellulose Fibers and Transparent Biocomposites Based on Oriented Holocellulose. *ACS Appl. Mater. Interfaces* **11**, 10310–10319 (2019).
42. celluloselab.com/price/Cellulose Lab Inc Product Price.htm. https://celluloselab.com/price/Cellulose%20Lab%20Inc%20Product%20Price.htm.